



JGR Biogeosciences

RESEARCH ARTICLE

10.1029/2019JG005297

Key Points:

- The ability to anticipate the timing of late spring phenological events using the timing of early-season heat is variable across the United States
- Locations exhibiting strong relationships between the timing of early-season and later-season thresholds vary by base temperature
- As the season progresses, relationships between the timing of heat accumulation thresholds increase

Supporting Information:

- Supporting Information S1

Correspondence to:

T. M. Crimmins,
theresam@u.arizona.edu

Citation:

Crimmins, M. A., & Crimmins, T. M. (2019). Does an early spring indicate an early summer? Relationships between intraseasonal growing degree day thresholds. *Journal of Geophysical Research: Biogeosciences*, 124, 2628–2641. <https://doi.org/10.1029/2019JG005297>

Received 5 JUN 2019

Accepted 2 AUG 2019

Accepted article online 23 AUG 2019

Published online 31 AUG 2019

Does an Early Spring Indicate an Early Summer? Relationships Between Intraseasonal Growing Degree Day Thresholds

M. A. Crimmins¹ and T. M. Crimmins^{2,3}

¹Department of Environmental Science, University of Arizona, Tucson, AZ, USA, ²School of Natural Resources and the Environment, University of Arizona, Tucson, AZ, USA, ³National Coordinating Office, USA National Phenology Network, Tucson, AZ, USA

Abstract Spring heat accumulation plays a major role in the timing of events such as leaf-out, leaf expansion, flowering, and insect hatch in temperate systems. Accordingly, heat accumulation can serve as a proxy for the timing of plant and insect phenological activity and can be used in a predictive way when the timing of heat accumulation thresholds being reached can be anticipated. This has strong value for a host of planning and management applications. If relationships exist between earlier- and later-season thresholds at a location, then the timing of later-season phenological events that are forced by the accumulation of warmth could be anticipated based on when earlier-season thresholds are met. Using high-resolution daily temperature data, we calculated the coherence in pairs of spring-season heat accumulation (growing degree day) threshold anomalies over 1948–2016. Overall, relationships between thresholds spanning the entire spring season were relatively low, while later season thresholds exhibited much higher correlations. This pattern is generally the result of decreasing variability in heat accumulation with season progression. However, correlation strengths did not follow latitudinal or gradients, revealing that within-season heat accumulation and interannual variability in threshold timing are unique to the specified base temperature and thresholds being compared. We show that the relationships between earlier- and later-season heat accumulation thresholds were sufficient to accurately predict the timing of phenological events in plants in two case examples.

Plain Language Summary In several recent years, spring has arrived especially early across much of the United States. Warm temperatures occurred earlier than average, and consequently, many trees and crops put on leaves or flowered days or weeks ahead of normal. Whether an early start to spring season weather conditions—and subsequently, plant and insect activity—leads to similarly early initiation of later-season events in plant and insect life cycles is not well understood. In some locations in the United States, the timing of the arrival of warm spring temperatures is a strong predictor of when biological events that occur in the middle and later part of spring would occur: an early start to spring will mean that later events will continue to occur ahead of schedule. In many other locations, the relationship is not as strong. These findings are important for scheduling management activities later in the season. For example, insect pest managers might use information regarding whether warm temperatures in the beginning or middle of spring are occurring ahead of schedule to plan whether crews should be dispatched earlier than usual.

1. Introduction

Anomalously early spring warmth and phenological activity typically draws a great deal of attention; for example, the particularly early spring in much of the United States in 2017 dominated news media for weeks. Often, declarations of “early spring” are based on anomalously warm winter and spring temperatures, resulting in earlier-than-normal activity among species and phenological events representing in the leading edge of the spring season (Ault et al., 2013; Ellwood et al., 2013; Hufkens et al., 2012). Whether an early start to spring season weather conditions—and subsequently, plant and animal activity—persists through the spring season, leading to early onsets of biological events occurring later into the season, has been less thoroughly evaluated.

In much of the Northern Hemisphere, spring heat accumulation plays a major role in the timing of events such as leaf-out, leaf expansion, flowering, and insect hatch (Cook et al., 2012; Crimmins et al., 2017; Schwartz et al., 2006; Vitasse et al., 2011). While other variables such as accumulated chill and daylength clearly play a role in influencing the timing of phenological events, accumulated warmth can often perform quite well at estimating spring-season phenological activity in temperate systems (Basler, 2016; Cook et al., 2012; Hufkens et al., 2018; Hunter & Lechowicz, 1992; Linkosalo et al., 2006). The strong performance of accumulated heat as an indicator of the timing of spring-season plant and insect activity has been long accepted and well-documented for many species (e.g., Arnold, 1959; Croft et al., 1976; Cross & Zuber, 1972; Herms, 2004; Hoover, 1955; Laskin et al., 2019; Melaas et al., 2016; Perry et al., 1986; Réaumur, 1735). Essentially, springtime physiological development commences once the average daily temperature surpasses a base threshold unique to the species, after which development increases as a function of local air temperature (Snyder et al., 1999). For many species, the specific amount of accumulated heat above a lower temperature threshold that is required to trigger a life cycle event, such as leaf out or adult emergence, has been quantified (e.g., Campbell et al., 1974; Herms, 2004; Murray, 2008, Cornell Cooperative Extension, 2010).

Spring-season heat accumulation does not happen at a constant rate: warmth accumulates rapidly during warm spells and stalls out during cold periods. Applying the logic that heat accumulation can serve as a proxy for the timing of plant and insect phenological activity, phenological events may happen earlier or later than average in a particular year, based on the weather in a season and when various heat accumulation thresholds are met at a location.

Within a season, heat accumulation can be consistently ahead or behind schedule, resulting in anomalies for two thresholds (in terms of difference in days from average date of occurrence) exhibiting the same sign—or exhibiting reverse signs—reflecting jumps and lags in heat accumulation based on weather variability occurring prior to the threshold dates (Figure 1a). For example, in 2018, consistent signs in anomalies were apparent between the USA National Phenology Network (USA-NPN)'s Spring Leaf and Bloom Indices, two heat-driven, early-season metrics (Ault et al., 2015; Schwartz et al., 2006), in much of the Upper Midwestern United States (both indices reached later than average) and Southwest (both indices reached earlier than average; Figures 1b and 1c). In contrast, anomaly direction and magnitude between these two indices varied dramatically in the Southeast as well as in parts of the Central Plains and the Pacific Northwest in 2018.

If relationships exist between earlier- and later-season thresholds at a location, then the timing of later-season phenological events that are forced by the accumulation of warmth could be anticipated based on when earlier-season thresholds are met. The ability to anticipate whether later-season events are likely to occur ahead or behind schedule based on early-season temperature conditions can guide a host of planning and management applications. For example, planning and scheduling activities related to the start and duration of the allergy season, harvest dates, pest and pathogen detection, invasive species management, and seasonal activities focused on biological events like peak bloom could all be enhanced with this form of insight (Enquist et al., 2014). Demand for information and ecological forecasts at multiple time scales is growing considerably among natural resource managers to guide planning and anticipate change (Bradford et al., 2018; Dietze et al., 2018). This information could serve as a valuable complement to seasonal and shorter-term weather and phenology forecasts (Carillo et al., 2018; Kirtman et al., 2014; Mo & Lettenmaier, 2014; Saha et al., 2014).

In this study, we explored whether the anomaly of earlier-season heat accumulation thresholds propagated to later-season thresholds, and whether the consistency in these anomalies varied across geography in the conterminous United States. We ask, if early-season spring warmth arrives ahead of (or behind) schedule, resulting in earlier-than-average (or later-than-average) phenological activity at the start of the season, will later-season heat-driven events similarly occur earlier (or later) than normal? Further, do the strength of these relationships vary across the conterminous United States?

In the northern hemisphere, the arrival of spring warmth progresses following latitude as Sun angle increases (Stine et al., 2009). Further, weather, and therefore, temperature accumulation, is more variable in the earliest months of the year and decreases as the spring and summer seasons progress due to changes in atmospheric circulation (James & Arguez, 2015; McKinnon et al., 2016; Stine & Huybers, 2012).

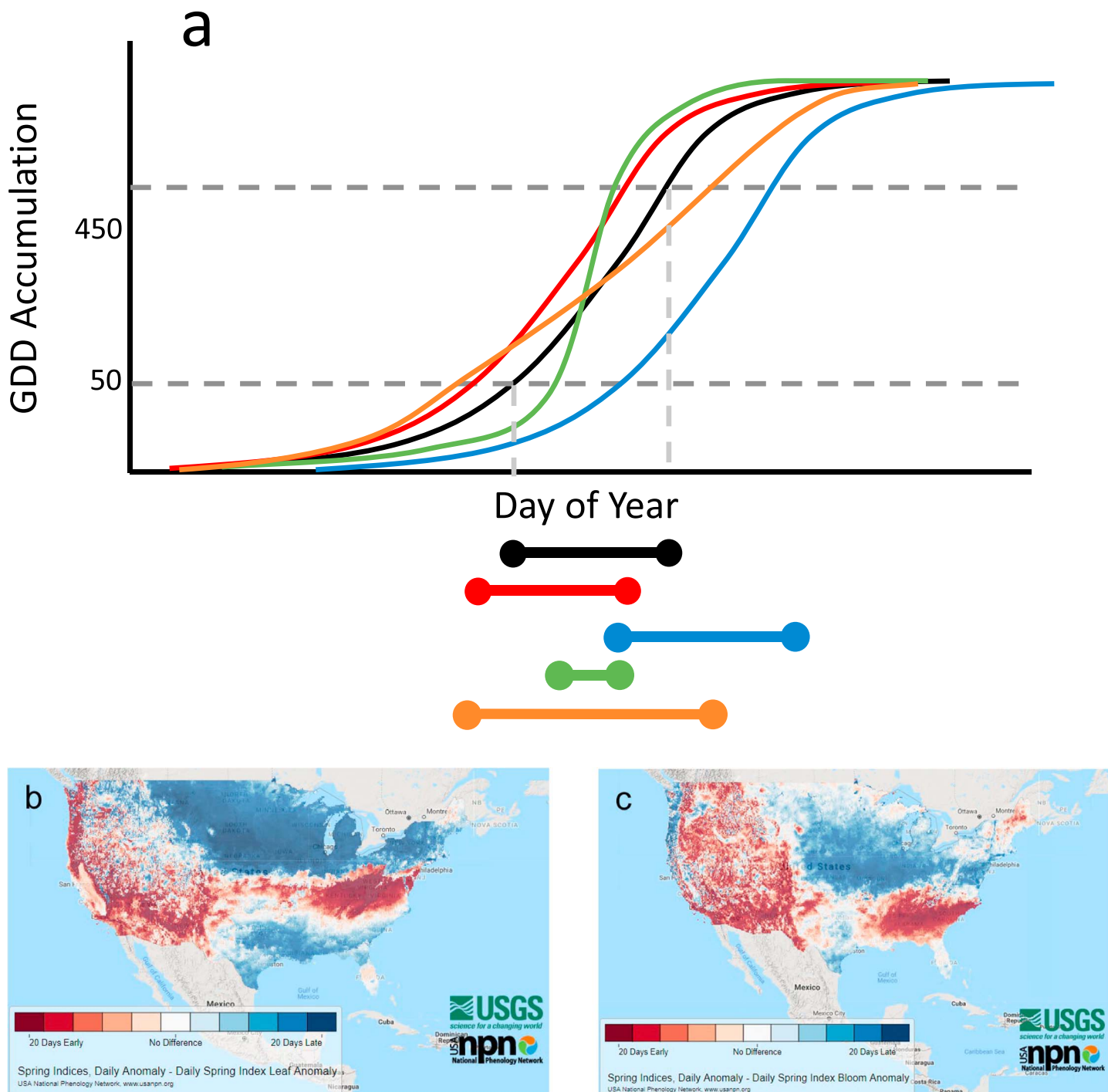


Figure 1. (a) Idealized heat accumulation curves, (b) 2018 Spring Leaf Index anomaly, and (c) 2018 Spring Bloom Index anomaly. When comparing two heat accumulation thresholds (a), both can be met early (red line), both thresholds being met late (blue line), and thresholds can be met both early and late (green and orange lines) compared to average conditions (black line). (b and c) Maps produced by the USA National Phenology Network (2018a, 2018b).

Accordingly, we anticipate that comparisons of later-season thresholds will exhibit stronger relationships than comparisons involving earlier-season thresholds. Additionally, we predict that within a comparison of two thresholds, correlation strength will increase with increasing latitude and elevation due to thresholds being met later in the year.

2. Materials and Methods

To evaluate intraseasonal relationships of the spring development period in plants and animals, we examined three thresholds in spring-season heat accumulation: 50, 250, and 450 growing degree days (GDDs) calculated in Celsius, based on a 1 January start date and two commonly used base temperatures 0 °C and 10 °C (Herms, 2004; Tait, 2008; Yang et al., 1995). Both 0 °C and 10 °C are common base temperatures in agriculture, turf management, and integrated pest management applications (Alessi & Power, 1971; Cardina et al., 2011; Cross & Zuber, 1972; Herms, 2004; Roby & Matthews, 2004; Wolfe et al., 1989) as well as phenological models (e.g., Heide, 1993; Raulier & Bernier, 2000; Ruml et al., 2010). These heat accumulation thresholds encompass the initiation of spring-season plant activity including budburst, leaf out, and flowering in the majority of plant species in the United States (Cornell Cooperative Extension, 2010; Herms, 2004; Murray, 2008; University of California Statewide Integrated Pest Management Program, 2019), as these events are generally strongly driven by temperature (Basler, 2016; Cook et al., 2012; Linkosalo et al., 2006; Melaas et al., 2016; Polgar et al., 2014). When calculated using 10 °C base temperature, 50 GDD represents the earliest-season activities in plants (Herms, 2004); 50 GDD calculated on 0 °C reflects an even earlier point in the spring season in temperate forest ecosystems. The 250-GDD (10 °C base temperature) threshold represents a very active point in the season, around which many plants are initiating spring activity, and 450 GDD (10 °C base temperature) represents a point several weeks later in the season, around which many plant species are exhibiting flowering activity (Herms, 2004; Murray, 2008; University of California Statewide Integrated Pest Management Program, 2019).

We calculated cumulative GDDs for each grid cell in each year (1948–2016) using the TopoWx gridded climatic dataset resampled from 800 m to nominal resolution of 3 km (Oyler et al., 2014). Daily total growing degree days above 0 °C and 10 °C thresholds were calculated using the simple average method (McMaster & Wilhelm, 1997). The day of year (DOY) that the 50-, 250-, and 450-GDD thresholds were met were then determined from the cumulative growing degree grids. Locations greater than 2,750 m failed to consistently reach 450 GDDs with the 10 °C base temperature; these areas were masked from subsequent analysis. To determine yearly anomalies for each of the thresholds and each base temperature, we calculated the mean DOY each threshold was met over the climate normal period of 1981–2010 and then differenced this DOY layer from each yearly threshold DOY layer.

We detrended each pixel anomaly time series to remove linear trends over the historical record that might impact the intraseasonal correlations. Pairwise Pearson's r correlations were then calculated on the detrended anomaly time series for each combination of GDD threshold and base temperature, resulting in six sets of correlations: 50–250 GDD (“early season”), 250–450 GDD (“late season”), and 50–450 GDD (“full season”), each for 0 °C and 10 °C base temperatures.

To demonstrate how these correlations could be used in a management context, we made predictions of the timing of phenological events that typically occur around 450 GDD in individual years based on when 50- and 250-GDD thresholds were reached at a single location. We used the detrended time for an individual pixel to construct linear models of when 450 GDD DOY would be met based on when 50 or 250 GDD DOY was met.

We used observational phenology data maintained by the USA-NPN verify predictions of phenological activity in two case studies. The phenology data maintained by the USA-NPN are contributed by thousands of volunteers across the United States through the phenology observing program, *Nature's Notebook* (Rosemartin et al., 2014) and exhibit high accuracy and reliability (Fuccillo et al., 2015). We accessed “individual phenometrics” data using the USA-NPN’s Phenology Observation Portal for species with phenophases known to occur at approximately 450 GDD (10 °C base temperature), including staghorn sumac (*Rhus typhina*) and wild strawberry (*Fragaria virginiana*; USA National Phenology Network, 2019).

3. Results and Discussion

3.1. Intraseason Correlations Vary by Geography and Point in Season

Correlations between heat accumulation thresholds range from a minimum of 0.02 (50–450 GDD, 0 °C base temperature) to a maximum of 0.98 (250–450 GDD, 10 °C base temperature; Figure 2) across the conterminous United States; nearly all correlations are significant. No negative correlations emerged,

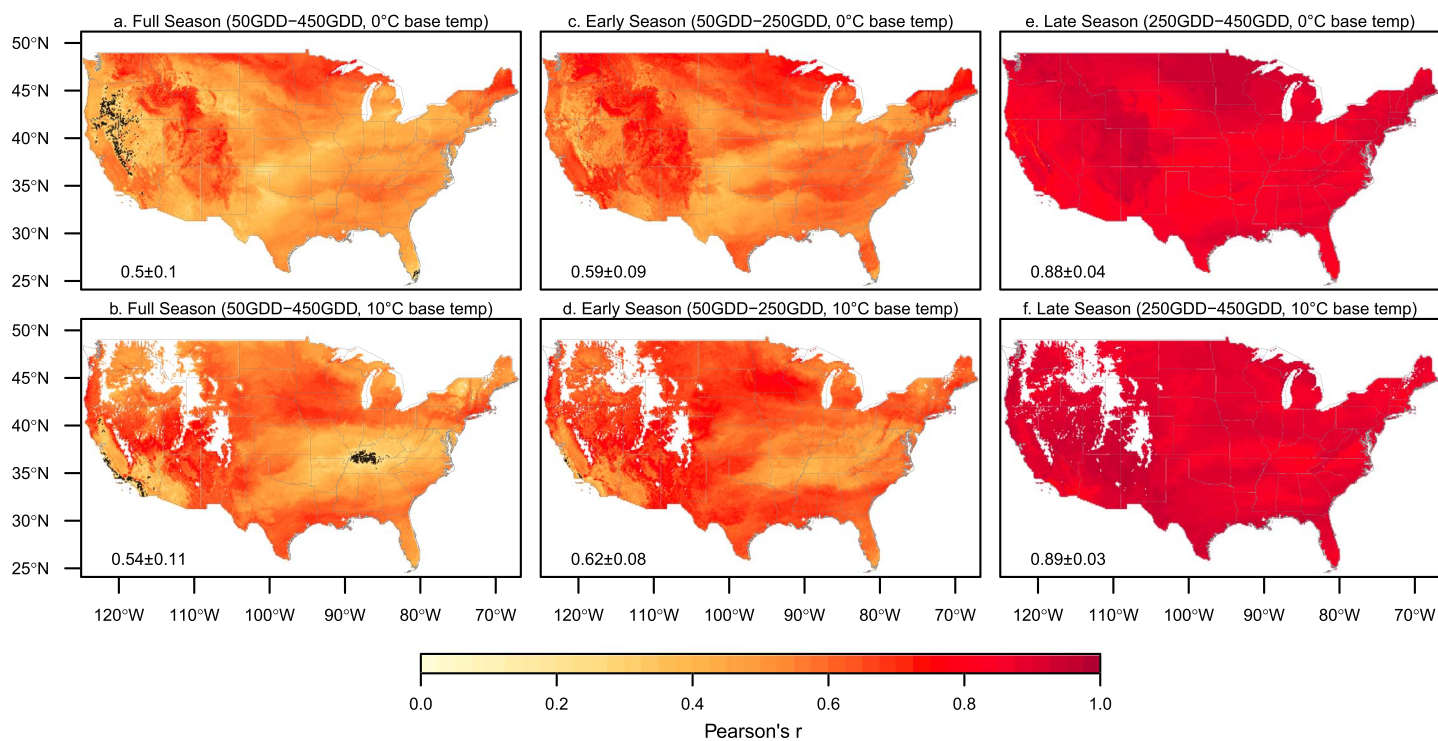


Figure 2. Pearson r correlations between detrended (a and b) 50–450 GDD, (c and d) 50–250 GDD, and (e and f) 250–450 GDD calculated using 0 °C and 10 °C base temperatures over period 1948–2016. Labels are correlation mean \pm SD. Nonsignificant correlations ($p > 0.05$) are shaded black.

indicating that there are no patterns where a negative anomaly for the first threshold consistently leads to a positive anomaly for the second threshold, and vice versa.

Correlation strengths are higher when later-season thresholds are compared, supporting our first hypothesis. The strongest relationships occur between the late-season thresholds (250 and 450 GDD; Figures 2a and 2b). Relationships between early-season (50 and 250 GDD; Figures 2c and 2d) as well as full-season (50 and 450 GDD; Figures 2e and 2f) thresholds are, overall, much weaker.

Patterns across geography and base temperatures are not as clear. Correlations between pairs of thresholds exhibit similar values when calculated using the two different base temperatures; however, in contrast to what we expected, the geographic patterns in the strength of the relationships vary and do not consistently follow latitudinal or topographic gradients (Figures 2a, 2c, and 2e versus Figures 2b, 2d, and 2f). Further, although correlations increase in strength when later-season thresholds are compared (Figure 2), the spatial pattern of the strength of the relationships is not held constant across multiple pairs of thresholds.

3.2. Threshold Timing and Variability Are Not Sufficient to Explain Correlations

Individual thresholds exhibit unique patterns in their timing and variability with which they occur from year to year. When combined, these variables underpin correlations between pairs of thresholds.

Following the established pattern that the arrival of spring warmth progresses with increasing latitude, the DOY 50-, 250-, and 450-GDD thresholds are met follow clear patterns: single thresholds are reached at later DOYs with increasing latitude and elevation (Figure S1). Thresholds calculated on 10 °C base temperature are reached weeks later than the same threshold calculated on 0 °C base temperature: the 450-GDD (0 °C base temperature) DOY map is roughly equivalent to the 50-GDD (10 °C base temperature) DOY map.

Patterns in the interannual variability of the DOY thresholds are met are also apparent, but not as straightforward. First, variability in threshold timing generally decreases as the season progresses: thresholds that occur later in the year vary less in their timing from year to year than those that are reached earlier in the year. This is true for both base temperatures, even though they occur weeks apart. The values

for the GDD450 variability in DOY (hereafter, SD (DOY)) maps (mean \pm SD: 7.7 ± 1.5 [base 0 °C], 7.1 ± 1.4 [base 10 °C]) are generally much lower than those for the GDD50 SD (DOY) maps (11.1 ± 5.3 [base 0 °C], 11.1 ± 2.9 [base 10 °C]; Figure S1). Second, with the exception of southern latitudes, locations that reach a threshold later in the year exhibit lower variability than locations that reach the same threshold earlier in the year. Low latitudes can exhibit very low variability in locations where daily average temperatures do not fall below the specified base temperature and heat accumulation therefore begins on the specified start date (e.g., 1 January). Finally, base temperature results in different geographic patterns in variability in threshold timing. Maps calculated on 0 °C base temperature show the largest variability at midlatitudes; the regions exhibiting the greatest variability on 10 °C base temperatures are notably lower latitudes.

These factors characterize the interannual variability in heat accumulation patterns, but alone they do not explain the geographic and temporal patterns in threshold correlation strengths observed in Figure 2. Rather, the degree of consistency in threshold anomalies is governed by whether the timing of the second threshold is advanced or delayed in concert with the first threshold. This relationship is reflected in two related factors: how much heat accumulation prior to the first threshold being met varies from year to year relative to how much the heat accumulation occurring between the thresholds varies from year to year. Thresholds “hang together”—that is, both occur earlier or later than average—when the variability in the duration between the two thresholds (SD (duration)) is less than the variability in the timing of the first threshold (SD(T_1)). Under these conditions, the timing of the first threshold may move around a great deal, shifting by many days from one year to the next, and the second threshold occurs at a relatively predictable span of time thereafter. As the variability in the two variables approach equal values, correlations decrease. Greater SD (duration) relative to SD(T_1) indicates that the anomaly direction of the second threshold does not regularly match that of the first threshold.

We present the relationship between these two variables as the ratio of SD (duration)/SD(T_1), where a value less than 1.0 reflects greater variability in the timing of the first threshold, a value equal to 1.0 represents similar variability in both metrics, and a value greater than 1.0 reflects greater variability in the duration of time between the thresholds. This pattern holds true across geography. Generally, when correlations are highest—and thresholds both occur either early or late—the values of this ratio are lowest (Figure 3). In this analysis, geographic patterns in threshold variability ratio values (Figure 4) closely match geographic patterns in the strength of correlations between thresholds (Figure 2).

To more clearly visualize the interplay between these two forms of variability and the concomitant correlations in threshold anomalies, we present time series of annual threshold dates and anomalies for several locations reflecting a diversity of onset dates, strength of full-season (50–450 GDD) correlations, and differences in correlations between base temperatures (Figure 5). In this figure, the DOY 50 and 450 GDD are met is provided in each of the 69 years by the filled circles. The variability in the timing of the first threshold, or SD(T_1), is reflected in leading (DOY 50 GDD) circles, and the variability in the duration between the two thresholds, or (SD (duration)), is reflected in the length of the bars connecting the DOY 50- and 450-GDD circles.

Location 3 (10 °C base temperature; Figure 5f) exhibits a pattern of greater SD(T_1) for 50 GDD than SD (duration)—seen as a large range of DOYs the 50-GDD threshold was met and comparatively low year-to-year difference in the duration of time between the thresholds being met. Accordingly, this location exhibits a threshold variation ratio of 0.72 and a comparatively high correlation. In contrast, an example of nearly equal variability in the two ratio variables (threshold variability ratio = 0.97) occurs at location 2 (10 °C base temperature; Figure 5d), indicating nearly equivalent measures of variability in the rate of heat accumulation prior to the first threshold being met and that occurring between the thresholds. This location exhibits a very low correlation, or weak ability to predict the timing of the second threshold based on the timing of the first threshold being met.

High threshold variation ratio values ($\gg 1.0$) occur at very high latitudes on the base 10 °C maps, where SD (duration) is much greater than SD(T_1). The comparatively very large variability in duration between the thresholds is the result of a short growing season and the onset of cool temperatures prior to the second threshold being met in some years, as in location 4 (10 °C base temperature; Figure 5h). At this location, the DOY 50 GDD that is met is comparatively consistent from year to year, and the duration of time between the thresholds being met is quite large. This phenomenon could also emerge at high latitudes with abbreviated growing seasons, with different choices of base temperatures or thresholds.

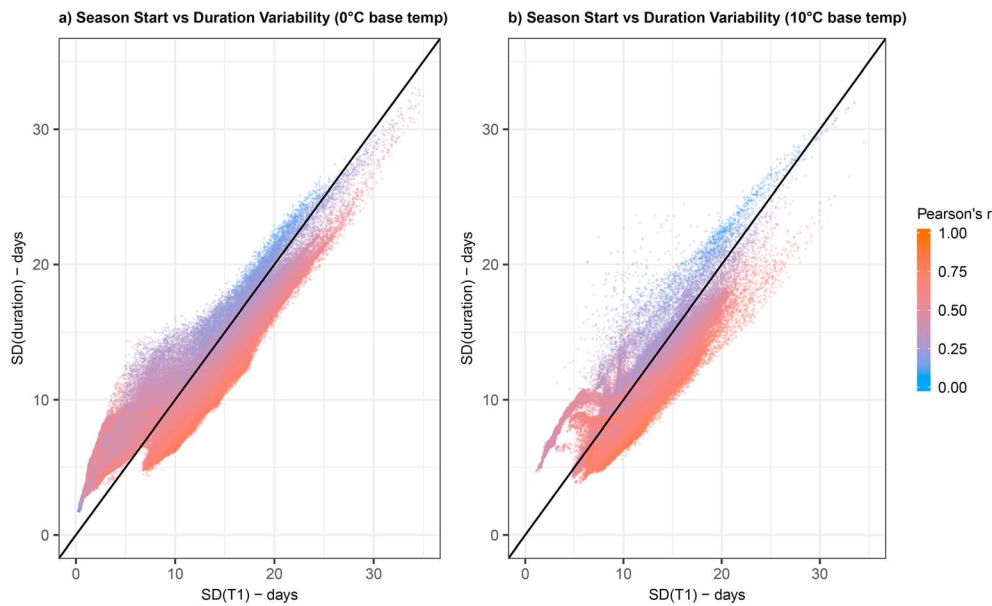


Figure 3. Pixel-wise relationship between the variability in the timing of the 50-GDD threshold ($SD(T1)$) and the variability in the 50- and 450-GDD thresholds ($SD(\text{duration})$) for (a) $0\text{ }^{\circ}\text{C}$ base temperature and (b) $10\text{ }^{\circ}\text{C}$ base temperature. Solid black line indicates 1:1 fit line. Color indicates the strength of Pearson's r correlation between 50- and 450-GDD threshold anomalies.

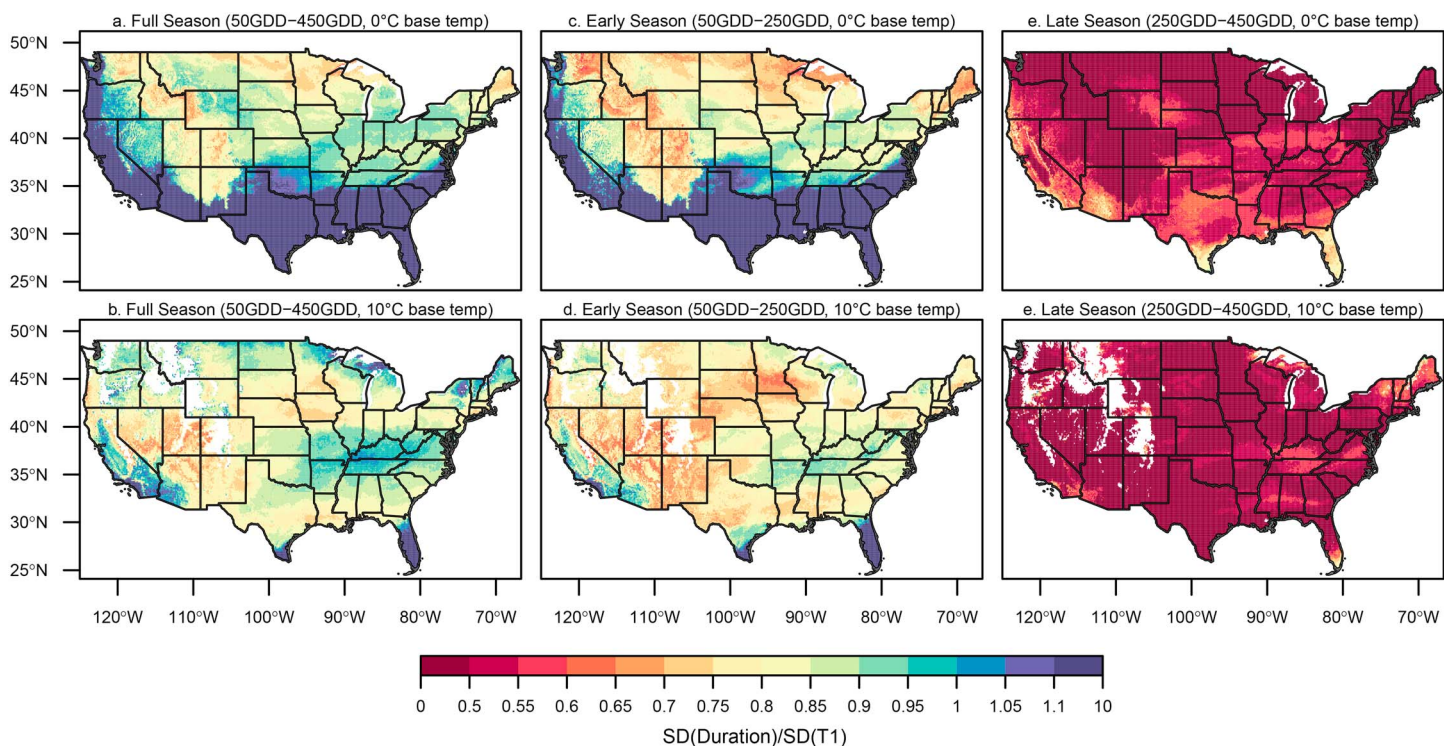


Figure 4. Threshold variability ratio values ($SD(\text{duration})/SD(T1)$), for (a and b) 50–450-GDD, (c and d) 50–250-GDD, and (e and f) 250–450-GDD comparisons calculated using $0\text{ }^{\circ}\text{C}$ and $10\text{ }^{\circ}\text{C}$ base temperatures.

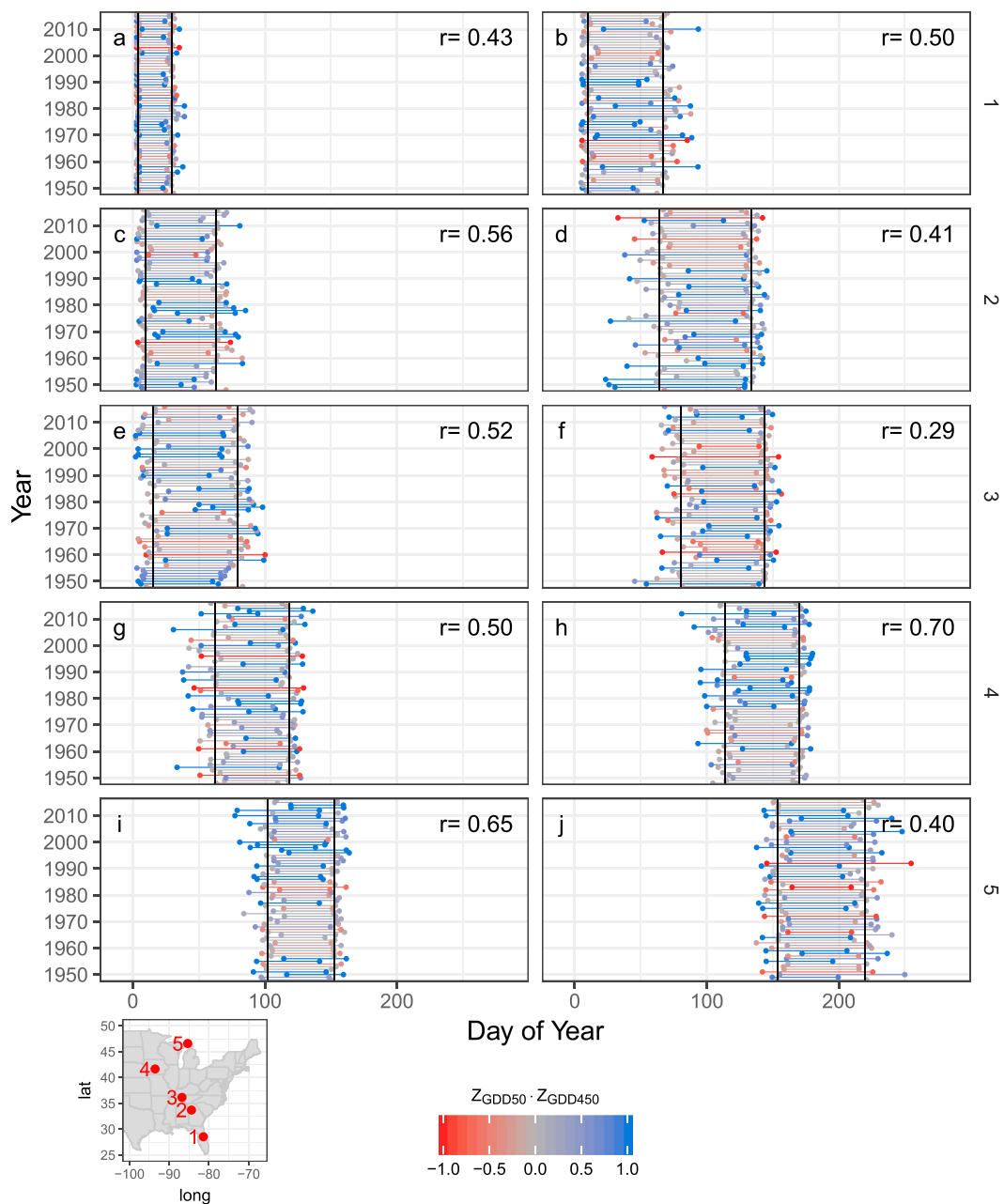


Figure 5. Timing of detrended 50- and 450-GDD thresholds at four locations in the continental United States calculated using (left column) 0 °C and (right column) 10 °C base temperatures. Filled circles that reflect the DOY 50 and 450 GDD were met and horizontal bars connecting the circles represent the duration of days between. Colors of bars represent the product of the threshold Z-scores and indicate consistency in anomalies (blue = both anomalies negative or positive; red = anomalies exhibit reverse signs). Long-term means of each threshold are represented by horizontal black line. Pearson r (top right corner), threshold variation ratio values (bottom right corner).

3.3. Geographic Limitations to Correlations

Aside from locations at high latitudes and elevations with short growing seasons, threshold variation ratio values greater than 1.0 at low latitudes indicate locations where temperature is not limiting, and correlation values can be artificially low or misleading. In locations where daily average temperatures do not fall below the specified base temperature, heat accumulation begins on the specified start date (e.g., 1 January). This results in lower variation for early thresholds being met compared to locations where heat

accumulation naturally begins on a date subsequent to the specified start date (Figure S1). The restricted range for the date of the first threshold impacts the true variability that could occur prior to 1 January possibly artificially reducing correlation values (Bland & Altman, 2011; Nie & Chu, 2011). Location 1 (Figure 5a; 0 °C base temperature) exhibits this phenomena. Variability in the DOY 50 GDD that is met at this location is very low (0.98 days; Figure 4), clearly lower than that of the duration between the two thresholds, and the result of daily average temperatures remaining above 0 °C year-round.

The geographic extent of locations with restricted range is a function of the base temperature selected. The 50–450-GDD comparison calculated on 10 °C base temperature yielded restricted ranges in southern Florida and Texas (Figure 4). Using a 0 °C base temperature for the same thresholds, the region impacted by this phenomenon stretches into all southern states as well as California and Oregon (Figure 4).

3.4. Correlation Strength Is a Product of Base Temperature, Thresholds Being Compared, and Within-Season Timing

The clearest pattern in the interseasonal threshold correlations is that correlations between later-season thresholds are notably higher than earlier-season thresholds (Figure 2). The greater coherence in later-season anomaly direction driving this relationship is explained by an overall decrease in heat accumulation variability as the season progresses (Figure S1), resulting in a shift toward greater $SD(T_1)$ relative to $SD(\text{duration})$. This shift is reflected in decreasing threshold variation ratio values (Figure 4).

Our second hypothesis—that correlations would increase with increasing latitude and elevation, as individual thresholds are met at progressively later DOYs with increasing latitude and elevation—was not supported; correlations do not show clear patterns following latitude or elevation (Figure 2). Following this logic, we might expect higher correlations for thresholds calculated using higher base temperatures, as thresholds calculated using higher base temperatures are reached later in the season (Figure S1). Again, this pattern is not apparent: the strength of correlations between the same two thresholds calculated on two base temperatures are very similar (Figure 2).

These findings underscore that the strength of the relationship between two heat accumulation thresholds at a particular location is not simply the result of the point in the year at which they are being reached. Rather, the consistency in threshold anomaly direction and magnitude, and therefore the ability to anticipate the timing of a later-season event based on earlier-season conditions, is specific to the base temperature and choice of thresholds under examination. The patterns in seasonal heat accumulation are unique to the specified base temperature. Further, the specifications for base temperature and thresholds evaluated govern the two forms of variability that indicate whether threshold anomalies are likely to consistently exhibit similar directions. The unique patterns in heat accumulation driven by local variability in daily temperatures between the thresholds do not follow predictable latitude or elevation patterns, even though the timing that thresholds are reached and the variability in this timing progress along these gradients.

Though not evaluated in this study, the choice of start date is likely to similarly affect the strength in threshold correlations. The choice of start date also dictates the pattern of heat accumulation and therefore the two forms of variability that comprise the threshold variation ratio and indicate whether threshold anomalies are likely to consistently exhibit similar directions.

3.5. Case Studies

Here we demonstrate how the relationships between thresholds could be used in real-world applications. We use the DOY the 50- and 250-GDD thresholds were met to predict the DOY 450 GDD would be met at various locations, including locations with observational phenology submitted by volunteer *Nature's Notebook* observers available that can be used to verify the relationships.

3.5.1. Predicting Sumac Flowering in Massachusetts to Support Honey Production

Staghorn sumac (*Rhus typhina*) flowers are an important pollen and nectar source for honeybees (Michigan State University Extension, 2018) and honey made from sumac flowers is appreciated for its mellow, rich flavor. Staghorn sumac anecdotally noted to flower around 450 GDD (base 10 °C). Knowing the timing of sumac flowering can guide beekeepers' activities, if honey made from sumac flowers is desired. *Nature's Notebook* observers track flowering phenology of staghorn sumac across the eastern United States.

On average, 450 GDD is reached on Grape Island in the Massachusetts Bay on DOY 183 (2 July, ± 4 day [standard deviation]). At this location, the correlation between 50 and 450 GDD is 0.66 and between 250 and 450 GDD is 0.87, offering information that could be leveraged in within-season forecasting.

In 2011, 50 GDD was met on DOY 125 (5 May), four days earlier than when this threshold is met at this location, based on the long-term average. Using this information, 450 GDD was predicted to be met at this location on DOY 182 (1 July)—one day earlier than normal—with a prediction interval of DOY 175–188. Subsequently, 250 GDD was met on DOY 160—three days earlier than normal for this location. Using this information, the prediction for 450 GDD was updated to DOY 181 (30 June), and the prediction interval narrowed to DOY 177–185. On Grape Island, 450 GDD was actually met on DOY 181. *Nature's Notebook* observers reported staghorn sumac in flower on DOY 179 (prior report of not yet in flower DOY 177). At this particular location, the timing of flowering was predicted accurately eight weeks in advance using the simple threshold correlation method.

The prediction worked similarly well at this location in 2012, a year with an exceptionally early start to the spring season. Using the DOY 50 GDD was met—DOY 110 (20 April), 18 days ahead of the long-term average—450 GDD was predicted to be met at this location seven days earlier than average—on DOY 176 (prediction interval DOY 169–183). Using the DOY 250 GDD was met (DOY 153), which was 10 days ahead of schedule, the prediction for 450 GDD remained at DOY 176 and the prediction interval narrowed to DOY 171–180. In actuality, 450 GDD was met at this location on DOY 177. Similarly, *Nature's Notebook* observers reported staghorn sumac in flower on DOY 173 (22 June) at this location (prior report of not yet in flower not in flower DOY 168).

3.5.2. Anticipating the Strawberry Harvest in Minnesota

Strawberries (*Fragaria* spp.) ripen around 450 GDD (base 10 °C; North Carolina State University Extension, 2016). Advance warning of whether this will occur early, on schedule, or late in a particular year can support scheduling crews to pick the berries. On average, 450 GDD is reached in Afton, MN, a prime strawberry-growing location, on DOY 179 (28 June, ± 6 days [standard deviation]). At this location, the correlation between 50 and 450 GDD is 0.70 and between 250 and 450 GDD is 0.89.

In 2017, another year with a very early start to spring, 50 GDD was met on DOY 115 (25 April), 10 days earlier than when this threshold is typically met at this location, based on the long-term average. Using this information, 450 GDD was predicted to be met at this location on DOY 174 (23 June)—five days earlier than normal—with a prediction interval of DOY 165–184. Subsequently, 250 GDD was met on DOY 148—11 days earlier than normal for this location. Using this information, the prediction for 450 GDD was updated to DOY 170 (19 June), and the prediction interval narrowed to DOY 163–175. At this location in Minnesota, 450 GDD was actually met on DOY 161 (10 June), 18 days earlier than normal. At this same location, *Nature's Notebook* observers reported that Virginia strawberries (*Fragaria virginiana*) ripe on DOY 159 (prior report of strawberries not yet ripe DOY 150).

In 2018, 50 GDD was met on DOY 124 (4 May), one day early. Using this information, 450 GDD was predicted to be met at this location one day early, on DOY 178 (prediction interval DOY 169–187). Following dramatic early-season warmth, 250 GDD was met on DOY 142, 17 days ahead of schedule, and the prediction for 450 GDD was updated to DOY 164 (prediction interval DOY 158–171). In actuality, 450 GDD was met at this location on DOY 150 (30 May), nearly a month early. *Nature's Notebook* observers reported that strawberries ripe on DOY 155 (prior report of strawberries not yet ripe DOY 151). In both 2017 and 2018, early-season warmth that resulted in the earlier-season thresholds to be reached ahead of schedule predicted an early arrival of 450GDD, though the magnitude of the advancement was too small.

3.5.3. Planning for Insect Pest Management Activities

Several pest insects, including azalea leafminer (*Caloptilia azaleela*), azalea whitefly (*Pealius azaleae*), oak skeletonizer (*Bucculatrix ainsliella*), pine needle miner (*Exoteleia pinifoliella*), rose chafer (*Macrodactylus subspinosus*), and spruce needle miner (*Endothenia albolineana*), reach a developmental stage at which control actions are effective at or around 450 GDD (base 10 °C; Cornell Cooperative Extension, 2010). We attempted to predict the timing of 450 GDD in 2018 at two locations: one where the correlations between earlier-season thresholds and the 450 GDD management threshold are high—near Des Moines, IA (Figure 2b), and another where they are low—near Nashville, TN (Figure 2b), to demonstrate how the intraseasonal threshold correlations could be used to inform management activities. In this example, we

do not have observational data to verify predictions. In Des Moines, on average, 54 days lapse between when 50 and 450 GDD are met, and in Nashville, this range is 64 days. Therefore, if the timing of 50 GDD being met can be used to anticipate when 450 GDD will be met, tree care specialists and natural resource managers have approximately eight-week advance warning of whether the event occurring at 450 GDD will be earlier or later than average in a particular year.

In Des Moines, the correlation between 50 and 450 GDD is 0.71 and between 250 and 450 GDD is 0.90, providing information that could be leveraged in within-season forecasting. On average, 450 GDD is reached in Des Moines on DOY 170 (19 June, ± 6 days). In 2018, 50 GDD was met in Des Moines on DOY 125, 11 days later than average for this location. Using this information, 450 GDD was predicted to be met at this location on DOY 173 (22 June)—two days later than normal—with a prediction interval of DOY 164–182. Following an unusually warm period, 250 GDD was met on DOY 146—four days earlier than normal for this location. Using this additional information, the prediction for 450 GDD was updated to DOY 166 (15 June)—five days earlier than average—and the prediction interval shifted to DOY 160–171. In Des Moines, 450 GDD was actually met on DOY 160 (9 June) in 2018.

In Nashville, the correlation between 50 and 450 GDD is 0.29 and between 250 and 450 GDD is 0.45. Because the correlation between 50 and 450 GDD is so low, we gain little by using it to make a prediction about when 450 GDD will occur. However, in this location, the DOY 250 GDD is met can still be used to give some predictive information regarding when 450 GDD will occur. At this location, 250 GDD was met in 2018 on DOY 94 (4 April), 28 days earlier than average. Using this information, 450 GDD was predicted to be met at this location on DOY 124 (4 May)—20 days earlier than normal—with a prediction interval of DOY 117–131. At this location, 450 GDD was actually met on DOY 124 (4 May) in 2018, the date that was predicted four weeks previous.

3.6. Implications and Limitations

Overall, relationships involving early-season thresholds are relatively weak across base temperatures. Mean correlations for these comparisons are around 0.5, indicating that only about one quarter of the variance in the timing of the second threshold is explained by the timing of the first threshold. However, higher full-season correlations, up to $r \sim 0.8$, exist at some locations such as higher elevations in the western United States when calculated using 0 °C base temperature. These locations offer greater promise for anticipating the timing of later-season events based on early-season temperature conditions. Relationships between later-season thresholds (250–450 GDD) are much stronger across the country. Many plant and animal species commence phenological activity, including first bloom, full bloom, egg hatch, and adult emergence at or near 250 GDD (10 °C base temperature); many other species undergo such events near or beyond 450 GDD (e.g., Cardina et al., 2011; Cornell Cooperative Extension, 2010; Herms, 2004; Murray, 2008; Wu et al., 2013). Accordingly, the timing of midseason heat accumulation thresholds can offer valuable information regarding whether later-season events may be expected to occur earlier or later than expected. This information may be especially useful for planning management activities when used in conjunction with seasonal and shorter-term forecasts. Future research could investigate the weather patterns driving the geographic patterns in the strength of relationships between earlier- and later-season thresholds. A deeper understanding of the drivers to these patterns on a regional scale would further enhance predictive capacity.

This analysis demonstrates that the choice of base temperature can have a strong impact on the strength of correlations between two thresholds. The base temperature is the temperature below which accumulated heat units are biologically irrelevant to species and phenological event of interest; this baseline varies by species and possibly also by phenophase (Klosterman et al., 2018; Wang, 1960). Applying heat accumulation threshold correlations in practical applications in a meaningful way necessitates using base temperatures appropriate to the species and life cycle events of interest. Our case studies demonstrate that this simple approach, when applied using suitable thresholds and base temperatures, can provide additional information regarding when events may occur later in the season and can enhance scheduling and planning decisions.

The utility in using correlations between heat accumulation thresholds to predict the timing of phenological events applies best to events that are cued primarily by winter and spring-season accumulated warmth. Accumulated temperature performs well to predict phenological transitions such as leaf-out and flowering

as well as later-spring and summer phenophases in many species (Basler, 2016; Melaas et al., 2016; Olsson & Jönsson, 2014; Yu et al., 2016). However, many phenological events are also cued by additional variables such as vernal chilling, daylength, and soil moisture (Flynn & Wolkovich, 2018; Polgar et al., 2014; Seyednasrollah et al., 2018); temperature threshold correlations could help with prediction, but will ultimately be insufficient to anticipate the timing for these events.

In this analysis, we chose to evaluate relationships among 50, 250, and 450 GDD, as these thresholds encompass the portion of the growing season during which accumulated temperature plays the greatest role in forcing phenological events. The approach undertaken here could be applied using any two thresholds to evaluate the predictive capacity between two points in the season. Future work could entail building a tool to calculate relationships between any selected thresholds on any base temperature for a location. However, as the growing season progresses into summer and autumn, variables such as photoperiod or accumulated chill can play a larger role in driving phenology (Delpierre et al., 2009; Richardson et al., 2013; Xie et al., 2018) and this approach may not represent phenological activity as well as in the spring season.

4. Conclusions

Whether the timing of phenological events such as flowering or insect hatch occurring later in the spring season can be anticipated based on early-season temperature conditions has the potential to enhance a planning and scheduling for a wide range of management activities, especially when combined with seasonal and shorter-term forecasts. We found that comparisons involving early-season thresholds were low. Correlation strength increased thresholds occurring farther into the spring season were compared, indicating that the timing of midseason heat accumulation thresholds can offer valuable information regarding whether later-season events may be expected to occur earlier or later than expected. These findings represent a form of ecological forecasting that might enhance intraseasonal planning decisions, addressing a need that is becoming widely recognized (Bradford et al., 2018; Dietze et al., 2018).

Acknowledgments

The mean DOY (1981–2010) 50-, 250-, and 450-GDD threshold DOY layers calculated in this analysis are available from the Dryad Digital Repository: <https://doi.org/10.5061/dryad.pp045j3>. The authors declare no conflicts of interest. We thank the staff of the USA National Phenology Network National Coordinating Office for inspiring this line of inquiry. This work was supported in part by the National Oceanic and Atmospheric Administration's Regional Integrated Sciences and Assessments (RISA) program through grant NA17OAR4310288 with the Climate Assessment for the Southwest program at the University of Arizona. We also thank Rey Granillo and Leland Boeman, University of Arizona Institute for the Environment, for computing resources used in this study. Computing resources provided by CyVerse were also utilized in this study (National Science Foundation under awards DBI-0735191 and DBI-1265383; www.cyverse.org). Staghorn sumac and strawberry phenology observational data were provided by the USA National Phenology Network and the many participants who contribute to its *Nature's Notebook* program. Finally, we thank two anonymous reviewers and the Associate Editor for their constructive comments that helped improve this manuscript.

References

- Alessi, J., & Power, J. F. (1971). Corn emergence in relation to soil temperature and seeding depth 1. *Agronomy Journal*, 63(5), 717–719. <https://doi.org/10.2134/agronj1971.00021962006300050018x>
- Arnold, C. Y. (1959). The determination and significance of the base temperature in a linear heat unit system. *Proceedings of American Society for Horticultural Science*, 74, 430–445.
- Ault, T. R., Henebry, G. M., de Beurs, K. M., Schwartz, M. D., Betancourt, J. L., & Moore, D. (2013). The false spring of 2012, earliest in North American record. *Eos, Transactions American Geophysical Union*, 94(20), 181–182. <https://doi.org/10.1002/2013EO200001>
- Ault, T. R., Schwartz, M. D., Zurita-Milla, R., Weltzin, J. F., & Betancourt, J. L. (2015). Trends and natural variability of North American spring onset as evaluated by a new gridded dataset of spring indices. *Journal of Climate*, 28(21), 8363–8378. <https://doi.org/10.1175/JCLI-D-14-00736.1>
- Basler, D. (2016). Evaluating phenological models for the prediction of leaf-out dates in six temperate tree species across central Europe. *Agricultural and Forest Meteorology*, 217, 10–21. <https://doi.org/10.1016/j.agrformet.2015.11.007>
- Bland, J. M., & Altman, D. G. (2011). Correlation in restricted ranges of data. *BMJ*, 342(mar11 1), d556. <https://doi.org/10.1136/bmj.d556>
- Bradford, J. B., Betancourt, J. L., Butterfield, B. J., Munson, S. M., & Wood, T. E. (2018). Anticipatory natural resource science and management for a changing future. *Frontiers in Ecology and Evolution*, 16(5), 295–303. <https://doi.org/10.1002/fee.1806>
- Campbell, A., Frazer, B. D., Gilbert, N., Gutierrez, A. P., & Mackauer, M. (1974). Temperature requirements of some aphids and their parasites. *Journal of Applied Ecology*, 11(2), 431–438. <https://doi.org/10.2307/2402197>
- Cardina, J., Herms, C. P., & Herms, D. A. (2011). Phenological indicators for emergence of large and smooth crabgrass (*Digitaria sanguinalis* and *D. ischaemum*). *Weed Technology*, 25(1), 141–150. <https://doi.org/10.1614/WT-D-10-00034.1>
- Carillo, C. M., Ault, T. R., & Wilks, D. S. (2018). Spring onset predictability in the North American Multimodel Ensemble. *Journal of Geophysical Research: Atmospheres*, 123, 5913–5926. <https://doi.org/10.1029/2018JD028597>
- Cook, B. I., Wolkovich, E. M., & Parmesan, C. (2012). Divergent responses to spring and winter warming drive community level flowering. *Proceedings of the National Academy of Sciences of the United States of America*, 109(23), 9000–9005. <https://doi.org/10.1073/pnas.1118364109>
- Cornell Cooperative Extension (2010). Using growing degree days for insect pest management. <https://s3.amazonaws.com/assets.cce.cornell.edu/attachments/1870/Using-Growing-Degree-Days-for-Insect-Pest-Management.pdf?1408019830>
- Crimmins, T. M., Crimmins, M. A., Gerst, K. L., Rosemarin, A. H., & Weltzin, J. F. (2017). USA National Phenology Network's volunteer-contributed observations yield predictive models of phenological transitions. *PLoS ONE*, 12(8), e0182919. <https://doi.org/10.1371/journal.pone.0182919>
- Croft, B., Howes, J. L., & Welch, S. M. (1976). A computer-based, extension pest management delivery system. *Environmental Entomology*, 5(1), 20–34. <https://doi.org/10.1093/ee/5.1.20>
- Cross, H. Z., & Zuber, M. S. (1972). Prediction of flowering dates in maize based on different methods of estimating thermal units. *Agronomy Journal*, 64(3), 351–355. <https://doi.org/10.2134/agronj1972.00021962006400030029x>
- Delpierre, N., Dufrene, E., Soudani, K., Ulrich, E., Cecchini, S., Boe, J., & Francois, C. (2009). Modelling interannual and spatial variability of leaf senescence for three deciduous tree species in France. *Agricultural and Forest Meteorology*, 149(6–7), 938–948. <https://doi.org/10.1016/j.agrformet.2008.11.014>

- Dietze, M. C., Fox, A., Beck-Johnson, L. M., Betancourt, J. L., Hooten, M. B., Jarnevich, C. S., et al. (2018). Iterative near-term ecological forecasting: Needs, opportunities, and challenges. *Proceedings of the National Academy of Sciences of the United States of America*, 115(7), 1424–1432. www.pnas.org/cdi/doi/10.1073/pnas.1710231115
- Ellwood, E. R., Temple, S. A., Primack, R. B., Bradley, N. L., & Davis, C. C. (2013). Record-breaking early flowering in the eastern United States. *PLoS ONE*, 8(1), e53788. <https://doi.org/10.1371/journal.pone.0053788>
- Enquist, C. A., Kellermann, J. L., Gerst, K. L., & Miller-Rushing, A. J. (2014). Phenology research for natural resource management in the United States. *International Journal of Biometeorology*, 58(4), 579–589. <https://doi.org/10.1007/s00484-013-0772-6>
- Flynn, D. F. B., & Wolkovich, E. M. (2018). Temperature and photoperiod drive spring phenology across all species in a temperate forest community. *The New Phytologist*, 219(4), 1353–1362. <https://doi.org/10.1111/nph.15232>
- Fuccillo, K. K., Crimmins, T. M., DeRivera, C., & Elder, T. S. (2015). Assessing accuracy in citizen science-based plant phenology monitoring. *International Journal of Biometeorology*, 59(7), 917–926. <https://doi.org/10.1007/s00484-014-0892-7>
- Heide, O. M. (1993). Daylength and thermal time responses of budburst during dormancy release in some northern deciduous trees. *Physiologia Plantarum*, 88(4), 531–540. <https://doi.org/10.1111/j.1399-3054.1993.tb01368.x>
- Herms, D. A. (2004). Using degree-days and plant phenology to predict pest activity. In V. Krischik & J. Davidson (Eds.), *IPM (integrated pest management) of Midwest landscapes*, Minnesota Agricultural Experiment Station Publication (pp. 49–59).
- Hoover, M. W. (1955). Some effects of temperature on the growth of southern peas. *Proceedings of the American Society for Horticultural Science USA*, 66, 308–312.
- Hufkens, K., Basler, D., Milliman, T., Melaas, E., & Richardson, A. D. (2018). An integrated phenology modelling framework in R. *Methods in Ecology and Evolution*, 9(5), 1276–1285. <https://doi.org/10.1111/2041-210X.12970>
- Hufkens, K., Friedl, M. A., Keenan, T. F., Sonnentag, O., Bailey, A., O'Keefe, J., & Richardson, A. D. (2012). Ecological impacts of a widespread frost event following early spring leaf-out. *Global Change Biology*, 18(7), 2365–2377. <https://doi.org/10.1111/j.1365-2486.2012.02712.x>
- Hunter, A. F., & Lechowicz, M. J. (1992). Predicting the timing of budburst in temperate trees. *Journal of Applied Ecology*, 29(3), 597–604. <https://doi.org/10.2307/2404467>
- James, R. P., & Arguez, A. A. (2015). On the estimation of daily climatological temperature variance. *Journal of Atmospheric and Oceanic Technology*, 32(12), 2297–2304. <https://doi.org/10.1175/JTECH-D-15-0086.1>
- Kirtman, B. P., Min, D., Infanti, J. M., Kinter, J. L. III, Paolino, D. A., Zhang, Q., et al. (2014). The North American Multimodel Ensemble: Phase 1 seasonal-to-interannual prediction; Phase 2 toward developing intraseasonal prediction. *Bulletin of The American Meteorological Society*, 95(4), 585–601. <https://doi.org/10.1175/BAMS-D-12-00050.1>
- Klosterman, S., Hufkens, S., & Richardson, A. D. (2018). Later springs green-up faster: The relation between onset and completion of green-up in deciduous forests of North America. *International Journal of Biometeorology*, 62(9), 1645–1655. <https://doi.org/10.1007/s00484-018-1564-9>
- Laskin, D. N., McDermid, G. J., Nielsen, S. E., Marshall, S. J., Roberts, D. R., & Montagh, A. (2019). Advances in phenology are conserved across scale in present and future climates. *Nature Climate Change*, 9(5), 419–425. <https://doi.org/10.1038/s41558-019-0454-4>
- Linkosalo, T., Häkkinen, R., & Hänninen, H. (2006). Models of the spring phenology of boreal and temperate trees: Is there something missing? *Tree Physiology*, 26(9), 1165–1172. <https://doi.org/10.1093/treephys/26.9.1165>
- McKinnon, K. A., Rhines, A., Tingley, M. P., & Huybers, P. (2016). The changing shape of Northern Hemisphere summer temperature distributions. *Journal of Geophysical Research: Atmospheres*, 121, 8849–8868. <https://doi.org/10.1002/2016JD025292>
- McMaster, G. S., & Wilhelm, W. W. (1997). Growing degree-days: One equation, two interpretations. *Agricultural and Forest Meteorology*, 87(4), 291–300. [https://doi.org/10.1016/S0168-1923\(97\)00027-0](https://doi.org/10.1016/S0168-1923(97)00027-0)
- Melaas, E. K., Friedl, M. A., & Richardson, A. D. (2016). Multiscale modeling of spring phenology across deciduous forests in the eastern United States. *Global Change Biology*, 22(2), 792–805. <https://doi.org/10.1111/gcb.13122>
- Michigan State University Extension (2018). Bee the best! <http://bees.msu.edu/staghorn-sumac/>
- Mo, K. C., & Lettenmaier, D. P. (2014). Hydrologic prediction over the conterminous United States using the National Multi-Model Ensemble. *Journal of Hydrometeorology*, 15(4), 1457–1472. <https://doi.org/10.1175/JHM-D-13-0197.1>
- Murray, M. (2008). Using degree days to time treatments for insect pests. *Utah State University Extension, IPM-05-08*.
- Nie, L., & Chu, H. (2011). Correlation in restricted ranges of data. *BMJ*, 342(mar11 1), d556. <https://doi.org/10.1136/bmj.d556>
- North Carolina State University Extension (2016). Reviewing growing degree day accumulations at Clayton. <https://strawberries.ces.ncsu.edu/2016/03/reviewing-growing-degree-day-accumulations-at-clayton/>
- Olsson, C., & Jönsson, A. M. (2014). Process-based models not always better than empirical models for simulating budburst of Norway spruce and birch in Europe. *Global Change Biology*, 20(11), 3492–3507. <https://doi.org/10.1111/gcb.12593>
- Oyler, J. W., Ballantyne, A., Jencso, K., Sweet, M., & Running, S. W. (2014). Creating a topoclimatic daily air temperature dataset for the conterminous United States using homogenized station data and remotely sensed land skin temperature. *International Journal of Climatology*, 35(9), 2258–2279. <https://doi.org/10.1002/joc.4127>
- Perry, K. B., Wehner, T. C., & Johnson, G. L. (1986). Comparison of 14 methods to determine heat unit requirements for cucumber harvest. *Horticultural Science*, 21, 419–423.
- Polgar, C., Gallatin, A., & Primack, R. B. (2014). Drivers of leaf-out phenology and their implications for species invasions: Insights from Thoreau's Concord. *The New Phytologist*, 202(1), 106–115. <https://doi.org/10.1111/nph.12647>
- Raulier, F., & Bernier, P. Y. (2000). Predicting the date of leaf emergence for sugar maple across its native range. *Canadian Journal of Forest Research*, 30(9), 1429–1435. <https://doi.org/10.1139/x00-064>
- Reaumur, R. A. F. (1735). Observations du thermomètre, faites à Paris pendant l'année 1735, comparées avec celles qui ont été faites sous la ligne, à l'Isle de France, à Alger et en quelques-unes de nos îles de l'Amérique. *Mémoires de l'Académie royale des sciences Paris*, 545–576.
- Richardson, A. D., Keenan, T. F., Migliavacca, M., Ryu, Y., Sonnentag, O., & Toomey, M. (2013). Climate change, phenology, and phenological control of vegetation feedbacks to the climate system. *Agricultural and Forest Meteorology*, 169, 156–173. <https://doi.org/10.1016/j.agrformet.2012.09.012>
- Roby, G., & Matthews, M. A. (2004). Relative proportions of seed, skin and flesh, in ripe berries from Cabernet Sauvignon grapevines grown in a vineyard either well irrigated or under water deficit. *Australian Journal of Grape and Wine Research*, 10(1), 74–82.
- Rosemarin, A. H., Crimmins, T. M., Enquist, C. A. F., Gerst, K. L., Kellermann, J. L., Posthumus, E. E., et al. (2014). Organizing phenological data resources to inform natural resource conservation. *Biological Conservation*, 173, 90–97. <https://doi.org/10.1016/j.biocon.2013.07.003>
- Ruml, M., Vuković, A., & Milatović, D. (2010). Evaluation of different methods for determining growing degree-day thresholds in apricot cultivars. *International Journal of Biometeorology*, 54(4), 411–422. <https://doi.org/10.1007/s00484-009-0292-6>

- Saha, S., Moorthi, S., Wu, X., Wang, J., Nadiga, S., Tripp, P., et al. (2014). The NCEP Climate Forecast System version 2. *Journal of Climate*, 27(6), 2185–2208. <https://doi.org/10.1175/JCLI-D-12-00823.1>
- Schwartz, M. D., Ahas, R., & Aasa, A. (2006). Onset of spring starting earlier across the Northern Hemisphere. *Global Change Biology*, 12(2), 343–351. <https://doi.org/10.1111/j.1365-2486.2005.01097.x>
- Seyednasrollah, B., Swenson, J. J., Domec, J. C., & Clark, J. S. (2018). Leaf phenology paradox: Why warming matters most where it is already warm. *Remote Sensing of Environment*, 209, 446–455. <https://doi.org/10.1016/j.rse.2018.02.059>
- Snyder, R. L., Spano, D., Cesarraccio, C., & Duce, P. (1999). Determining degree-day thresholds from field observation. *International Journal of Biometeorology*, 42(4), 177–182. <https://doi.org/10.1007/s004840050102>
- Stine, A. R., & Huybers, P. (2012). Changes in the seasonal cycle of temperature and atmospheric circulation. *Journal of Climate*, 25(21), 7362–7380. <https://doi.org/10.1175/JCLI-D-11-00470.1>
- Stine, A. R., Huybers, P., & Fung, I. Y. (2009). Changes in the phase of the annual cycle of surface temperature. *Nature*, 457(7228), 435–440. <https://doi.org/10.1038/nature07675>
- Tait, A. B. (2008). Future projections of growing degree days and frost in New Zealand and some implications for grape growing. *Weather Climate*, 28, 17–36. <https://doi.org/10.2307/26169696>
- University of California Statewide Integrated Pest Management Program (2019). <http://ipm.ucanr.edu/models/index.html>
- USA National Phenology Network (2018a). *Spring bloom index anomaly*. Tucson, AZ: USA National Phenology Network. <https://www.usanpn.org/files/pnpn/maps/six-bloom-index-anomaly.png>
- USA National Phenology Network (2018b). *Spring leaf index anomaly*. Tucson, AZ: USA National Phenology Network. <https://www.usanpn.org/files/pnpn/maps/six-leaf-index-anomaly.png>
- USA National Phenology Network (2019). Plant and animal phenology data. Data type: Status and intensity. 01/01/2009–05/11/2019 for continental U.S. USA-NPN, Tucson, Arizona, USA. Data set accessed 11 May 2019 at. <http://doi.org/10.5066/F78S4N1V>
- Vitasse, Y., Francois, C., Delpierre, N., Dufrene, E., Kremer, A., Chuine, I., & Delzon, S. (2011). Assessing the effects of climate change on the phenology of European temperate trees. *Agricultural and Forest Meteorology*, 151(7), 969–980. <https://doi.org/10.1016/j.agrformet.2011.03.003>
- Wang, J. U. (1960). A critique of the heat unit approach to plant response studies. *Ecology*, 41(4), 785–790. <https://doi.org/10.2307/1931815>
- Wolfe, D. W., Albright, L. D., & Wyland, J. (1989). Modeling row cover effects on microclimate and yield: I. Growth response of tomato and cucumber. *Journal of the American Society for Horticultural Science*, 114, 562–568.
- Wu, L., Boyd, N. S., Cutler, C., & Olson, A. R. (2013). Spreading dogbane (*Apocynum androsaemifolium*) development in wild blueberry fields. *Weed Science*, 61(3), 422–427. <https://doi.org/10.1614/WS-D-12-00156.1>
- Xie, Y., Civco, D. L., & Silander, J. A. Jr. (2018). Species-specific spring and autumn leaf phenology captured by time-lapse digital cameras. *Ecosphere*, 9(1), e02089. <https://doi.org/10.1002/ecs2.2089>
- Yang, S., Logan, J., & Coffey, D. L. (1995). Mathematical formulae for calculating the base temperature for growing degree days. *Agricultural and Forest Meteorology*, 74(1–2), 61–74. [https://doi.org/10.1016/0168-1923\(94\)02185-M](https://doi.org/10.1016/0168-1923(94)02185-M)
- Yu, R., Schwartz, M. D., Donnelly, A., & Liang, L. (2016). An observation-based progression modeling approach to spring and autumn deciduous tree phenology. *International Journal of Biometeorology*, 60(3), 335–349. <https://doi.org/10.1007/s00484-015-1031-9>

